A new approach of MHD flows for UCM fluid over a permeable moving plate with space and temperature dependent internal heat generation/absorption

Cite as: AIP Conference Proceedings **2236**, 060002 (2020); https://doi.org/10.1063/5.0006834
Published Online: 20 May 2020

Jagadish Vaijinath Tawade, Mahadev Malikarjun Biradar, and Shaila Sangangouda Benal

A new approach of MHD flows for UCM fluid over a permeable moving plate with space and temperature dependent internal heat generation/absorption

Jagadish Vaijinath Tawade[1, a)], Mahadev Malikarjun Biradar[2, b)] and Shaila Sangangouda Benal[3, c)]

[1]*Department of Mathematics, Bheemanna Khandre Institute of Technology,Bhalki-585328, Karnataka, INDIA*
2 Department of Mathematics, Basaveshwar Engineering College (Autonomous), Bagalkot-587103, Karnataka, INDIA
[3]*Department of Mathematics, B.L.D.E.A's V. P. Dr. P. G. Halakatti College of Engineering and Technology, Vijayapur-586103, Karnataka, INDIA*

Corresponding Author: [a)]jagadishmaths22@gmail.com
[b)]mmbmh@becbgk.edu
[c)]shailabenal04@gmail.com

Abstract. Present paper investigates a new approach for the MHD boundary layer flow of an incompressible upper-convected Maxwell fluid over a permeable horizontal moving plate influenced by non-uniform heat source/sink parameter. We have reduced the governing PDE's into a kind of nonlinear ODE's using similarity transformations. These ODE's are solved with appropriate boundary conditions by efficient shooting with Runge-Kutta method. The obtained values are tabulated and compared with the earlier published papers.

Key words:PDE, ODE, elastic parameter, Prandtl number, porous medium, stretching sheet.

INTRODUCTION

The boundary layer flow over the permeable moving plate has broad range of applications in polymer processing units and metal processing units. For example, the manufacture of artificial sheets and foils involves the extrusion of molten polymers through a slit with the extrudate collected by a wind-up roll.Nevertheless, there be a situation that the artificial sheet is stretched without heat transfer, the artificial sheetsare elongated in certain directions for the improvement of its mechanical properties.Flow through a continuous moving plate has been studied by Sakiadis[1]. In the drawing of artificial sheets, the velocity is proportional and boundary layer thickness increases with the distance from the slit has studied by Crane[2]. Later, in the view on broad range of application over heat and mass transfer, several authors. [3-6] have investigated the flow under various parameters. It is also noted that,the few studies explain the flow ofUCM fluids. [7-11].

eTIME-2019 – International Conference on Emerging Trends in Mechanical Engineering
AIP Conf. Proc. 2236, 060002-1–060002-14; https://doi.org/10.1063/5.0006834
Published by AIP Publishing. 978-0-7354-1995-7/$30.00

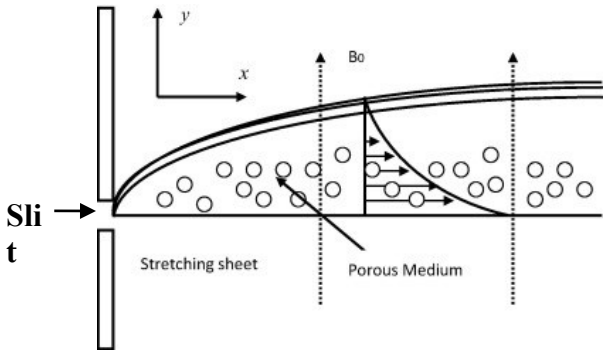

Figure 1. Schematic of porous stretching sheet.

The theory of permeability over a stretching sheet (schematic is shown in fig.1)is an important area that has paying a special attention of researchers due to its wide range of applications in various disciplines like civil engineering, mechanical engineering, petroleum engineering, food industry, and biomedical sciences. With the motivation of these industrial applications, the main purpose of the investigations is to estimate the flow of UCM fluid over permeable moving plate in occurrence of non-uniform heat source/sink. The projected fluid model is more general, the consideration of various combined effectmake the study quite versatile. The proposed BVP's are solved numerically using MATLAB bvp4c package. A proportional study between the existing with the available literature are tabulated, discussed and shown with the aid of graphs.

PROBLEM FORMULATION

We have considered the flow of UCM fluid flow over the porous moving plate at $y = 0$, the governing PDEs of the flow problem are given by

$$\frac{\partial u}{\partial x} + \frac{\partial u}{\partial y} = 0 \quad (1)$$

$$u\frac{\partial u}{\partial x} + v\frac{\partial u}{\partial y} + \beta\left(u^2\frac{\partial^2 u}{\partial x^2} + v^2\frac{\partial^2 u}{\partial y^2} + 2uv\frac{\partial^2 u}{\partial x \partial y}\right) = v\frac{\partial^2 u}{\partial y^2} - \frac{\sigma {B^2}_0}{\rho}\left(u + \lambda v\frac{\partial u}{\partial y}\right) \quad (2)$$

Where u & v represents horizontal and vertical velocities,β- relaxation time, B_0-magneticfield strength, ν-the kinematic viscosity,ρ - density of the fluid and σ-electrical conductivity. Assuming that stretching of the sheet is linear, the corresponding boundary conditions take the form as,

$$u = ax,\ v = V_s aty = 0 \quad (3)$$

$$u \to \infty \text{ as } y \to \infty \quad (4)$$

Here'a' is constant, negative values ofVsrepresents suction velocity, and positive values ofVsrepresents injection or blowing velocity. Let us introduce similarity variable η and stream function ψ as

$$\eta = y\sqrt{\frac{a}{v}},\ \psi = x\sqrt{va}\ \mathrm{f}(\eta) \quad (5)$$

Then the continuity Eqn.(1) satisfies the ψ defined as$u = \frac{\partial \psi}{\partial y}\&v = \frac{\partial \psi}{\partial x}\&$ Eqn.(2) becomes

$$f''' - M^2 f' + K(2ff'f'' - f^2 f''') - f'^2 + (1 + M^2 K)ff'' = 0 \quad (6)$$

Where $k = \lambda a$-Deborah number, magnetic field is $M^2 = \frac{\sigma {B^2}_0}{\rho a}$and R= $\frac{\mathrm{Vs}}{\sqrt{va}}$- Suctionvelocity /Injection velocity. The corresponding BC's are

$$f(\eta) = R,\ f'(\eta) = 1 \quad at\eta = 0 \quad (7)$$

$$f'(\eta) \to 0 \quad \text{as} \quad \eta \to \infty \quad (8)$$

The thermal boundary layer equation for the flow is as given below

$$u\frac{\partial T}{\partial x} + v\frac{\partial T}{\partial y} = \frac{k}{\rho C_p}\frac{\partial^2 y}{\partial x^2} + \frac{\mu}{\rho C_p}\left(\frac{\partial u}{\partial y}\right)^2 + \frac{q'''}{\rho C_p} \quad (9)$$

where T-temperature, $C_p$specific heat, at constant pressure, k- thermal conductivity and q'''-non-uniform heat source/sink is expressed as

$$q'''=\frac{ku_w(x)}{x\upsilon}[A^*(T_w-T_\infty)f'_\eta+B^*(T-T_\infty)]$$

Here space and temperature dependent heat transfer are respectively denoted by A^* and B^*. N egative values correspond to heat absorption and positive values corresponds to heat generation. The dimensionless temperature is defined as

$$\theta(\eta)=\frac{T-T_\infty}{T_w-T_\infty},\quad \text{where } T_w-T_\infty=b\left(\frac{x}{l}\right)^2\ \theta(\eta) \qquad (PST\ Case) \tag{10}$$

$$g(\eta)=\frac{T-T_\infty}{b\left(\frac{x}{l}\right)^2\frac{1}{k}\sqrt{\frac{\nu}{b}}},\ \text{where } T_w-T_\infty=\frac{D}{k}\left(\frac{x}{l}\right)^2\sqrt{\frac{\upsilon}{b}} \qquad (PHF\ Case) \tag{11}$$

The boundary conditions of thermal boundary layer equations depend upon the followingtwo cases namely,
(i) Surface temperature is prescribed (ii) Wall heat flux is prescribed

(i) PST-Case: The surface temperature is specified as quadratic and is given by

$$u=Bx,\ \ v=0,\quad T=T_w(x)=T_0-T_s\left(\frac{x}{l}\right)^2 \quad at\ y=0. \tag{12}$$

$$u=0,\qquad T\to T_\infty \qquad as \quad y\to\infty$$

Here characteristic length is *l,* the dimensionless temperature variable θ given by (10)satisfies by using (5), (9) and (12) as

$$\Pr\left[2f'\theta-\theta'f-Ecf''^2\right]=\theta''-(A^*f'+B^*\theta), \tag{13}$$

Where $\Pr=\frac{\mu c_p}{k}$ is the Prandtl number, $Ec=\frac{a^2l^2}{C_pT_s}$ is the Eckert number, A^* are space dependent and B^* is the temperature dependent heat transfer.The corresponding BCs are

$$\theta(\eta)=1 \quad \text{at} \quad \eta=0$$
$$\theta(\eta)\to 0 \ \ as\ \ \eta\to\infty \tag{14}$$

(ii). PHF-Case : Here wall surface is considered as a quadratic power of x in the form

$$u=Bx,\quad -k\left(\frac{\partial T}{\partial y}\right)_w=q_w=b\left(\frac{x}{l}\right)^2 \quad at \quad y=0 \tag{15}$$
$$u\to 0,\quad T\to T_\infty \quad as \quad y\to\infty.$$

The equation (10) byusing (5), (9) and (15), gives

$$\Pr\left[2f'g-g'f-Ecf''^2\right]=g''-(A^*f'+B^*g) \tag{16}$$

With BC's are

$$g'(\eta)=-1\ at\ \eta=0.\quad g(\eta)\to 0\ as\ \eta\to\infty. \tag{17}$$

For local Nusselt number is in dimensionless form defined as

$$Nu_x\equiv-\frac{x}{T_w-T_\infty}\left(\frac{\partial T}{\partial y}\right)_{y=0}=-x\sqrt{\mathrm{Re}}\ \theta'(0) \tag{18}$$

Similarly, skin-friction coefficientor frictional drag is

$$C_f\equiv\frac{\left(\mu\frac{\partial u}{dy}\right)_{y=0}}{\rho(Bx)^2}=-f''(0)\frac{1}{\sqrt{\mathrm{Re}_x}} \tag{19}$$

where $\mathrm{Re}_x=\frac{\rho Bx^2}{\mu}$ stands for local Reynolds number.

NUMERICAL SOLUTION

We implement the suitable shooting system with Runge-Kutta4th order scheme to solve the BVPs.. The transformed ODE's represented by equations (6) and (13) are transformed into following system.

$$\frac{df_0}{d\eta} = f_1, \quad \frac{df_1}{d\eta} = f_2, \quad \frac{df_2}{d\eta} = \frac{(f_1)^2 - (1+M^2K)f_0f_2 + M^2f_1 - 2Kf_0f_1f_2}{1-K(f_0)^2},$$

$$\frac{d\theta_0}{d\eta} = \theta_1, \quad \frac{d\theta_1}{d\eta} = \Pr[2f_1\theta_0 - \theta_1 f_0 - Ec(f'')^2] + (A^*f' + B^*\theta) \tag{20}$$

Subsequently the boundary conditions in (8) and (12) take the form,

$$f_0(0) = 0, \quad f_1(0) = 1, \quad f_1(\infty) = 0, \quad f_2(0) = 0, \quad \theta_0(0) = 0, \quad \theta_0(\infty) = 0. \tag{21}$$

Here $f_0 = f(\eta)$ and $\theta_0 = \theta(\eta)$, aforementioned BVP is first transformed into an IVP by properly guessing the neglected slopes $f_2(0)$ and $\theta_1(0)$. The resulting IVP's are solved with the help of MATLAB bvp4c package.

TABLE 1. $-f''(0)$ with $M = 0$ for different values of β

β	Sadeghy, Hajibeygi and Taghavi [13]	Hayat, Abbas and Sajid [14]	Existing Results
0.0	1.00000	1.90250	0.999961
0.4	1.10084	2.19206	1.101849
0.8	1.19872	2.50598	1.196690
1.2	-	2.89841	1.285255
1.6	-	3.42262	1.368640
2.0	-	4.13099	1.447616

TABLE 2. Ec and Mn in PST case ($\beta = 0.1,\ Pr = 3, A^* = B^* = 0.1$)

Ec	*Mn*	Aliakbar et. al [12] $-\theta'(0)$	Existing values $-\theta'(0)$
0.0	*0.0*	2.47116	1.227048
5.0	*0.0*	−1.38806	−0.718810
10.0	*0.0*	−5.24982	−2.665281

TABLE 3. $\theta(1)$ and $-\theta'(0)$ for different values of Pr,Ec, A*, B* and β .

Pr	*Ec*	*A**	*B**	β	$\theta(1)$	$\theta'(0)$
1					0.000000	-1.149181
5	0.2	0.1	0.1	0.1	-0.000001	-2.972451
10					-0.000001	-4.244380
	1				0.000000	-0.837850
1	2	0.1	0.1	0.1	-0.000001	-0.448685
	5				-0.000001	0.718812
		-0.1			0.000000	-1.265851
1	0.2	0.0	0.1	0.1	0.000000	-1.207516
		0.1			0.000000	-1.149180
			-0.1		0.000000	-1.252832
1	0.2	0.1	0.0	0.1	0.000000	-1.203613
			0.1		0.000000	-1.149180
				0.0	-0.000000	-1.163280
1	0.2	0.1	0.1	0.1	-0.000000	-1.149183
				0.3	-0.000000	-1.121013

RESULTS AND DISCUSSION

The obtained ODE's represented by equations (6), (13) and (16) with the corresponding BC's represented by (7), (8), (14) and (17) are evaluated with the help of Runge-Kutta fourth order and shooting system. Suitable conversion is taking up to convert the governing PDE's into a system of non-linear ODE's. The results are tabulated (Ref. Table 1, 2 & 3) for different values of local skin-friction and local Nusselt number, compared with references [12,13,14] and discussed in brief.

Figs 2 & 3 reveals that, for $R = 0.3$ and $K = 1$, increasing values of magnetic parameter M decreases the velocity profile of the fluid which causes decrease in the thickness of the boundary layer from the slit. This is due to the fact that the applied transverse magnetic field produces a drag in the form of Lorentz force in that way decreasing the magnitude of velocity profile.

Figures 4 and 5 are the graphical representations of the velocity profiles $f'(\eta)$ and $f(\eta)$, respectively, for various values of the suction/injection parameter. Analyzing these figures shows

that the general increase in the suction $R > 0$ causes the progressive reduction in the velocity $f'(\eta)$ and the corresponding thinning in the boundary layer thickness, while the reverse is true for the injection.

Figs. 6 & 7 represent that, β effects on f, it is observed that enhancing in the values of β which reduces horizontal and vertical velocities above the plate. Also, Figs. 8 & 9 represents for rising values in β predicts reducing in the total amount of heat transfer from the moving plate. That is, higher values in β reduces temperature of the fluid above the moving plate.

Figs.10 & 11 represents that, for raise in the values of Pr is observed to reduce the thermal parameter. i.e., the thermal boundary layer becomes thinner for higher the Pr. Thus, raising value in the Pr parameter found the rate of thermal diffusion drops in both PST and PHF cases. For PST case the dimensionless wall temperature is 1 for all parameter values.

Figs. 12 & 13 represent that, for enhancing in the values of Ec enhances the thermal parameter for both PST and PHF cases. The effect of viscous dissipation is to enhance the temperature in the fluid film. i.e., increasing values of Ec contributes in thickening of thermal boundary layer.

Figs. 14 & 15 represent the thermal property effects for PST and PHF cases respectively for special values of A^*. For positive values of A^*, it generates the energy in the boundary region which is the basis for enhancing the thermal parameter across PST and PHF cases. For negative values of A^* which absorb the thermal parameter across PST and PHF cases.

Figs. 16 & 17 represent the thermal property effects for PST and PHF cases respectively for special values of B^*. The result of B^* is alike to that for A^*. The effect of sink parameter ($A^* < 0$, $B^* < 0$) reduces the temperature in the fluid as the effect of source parameter ($A^* > 0$, $B^* > 0$) enhances the temperature. Heat sink is preferred for effective cooling of the sheet.

CONCLUSIONS

In this paper, an analysis has been carried out on the effect with space and temperature dependent internal heat generation/absorption over a flat porous moving plate for the UCM fluid. We observe the following.

Reduce in the velocity profile due to raise in the strength of magnetic field and raise in elastic parameter reduces velocity of fluid flow. These effects overall is to suppress the velocity field above the stretching sheet, which is the basis for enrichment of the thermal effects.

Skin friction coefficient increases with M and K.

An increase in β, there is a decline in velocity field. The effect of β on the UCM fluid over a permeablehorizontal moving plate is to suppress the velocity in the boundary region, which is the basis for enrichment of the thermal effects.

An increase in Pr depicts in declining the thermal parameter across PST and PHF cases.

Raise in the Ecwill be the basis for raise in the thermal parameter, which causes reduce in the rate of cooling.

The effect of space and temperature dependent internal heat generation / absorption is to cause temperature for rising positive values and absorb temperature for falling negative values.

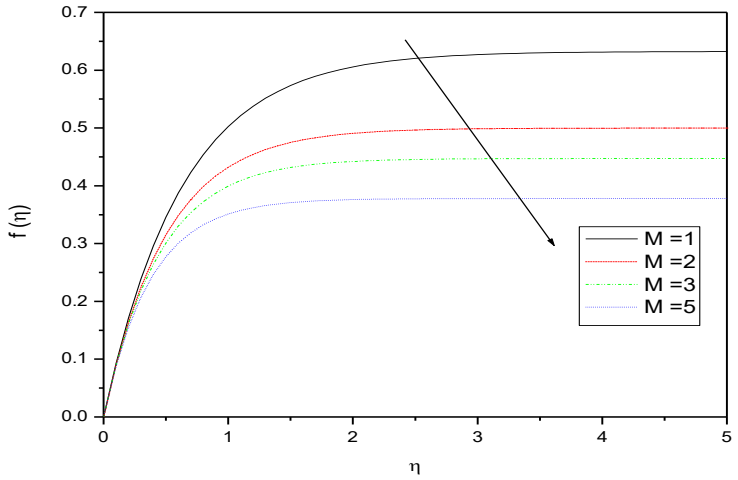

Figure 2. Horizontal variation of Mwhen porous parameter $K = 1$ and $R = -0.3$

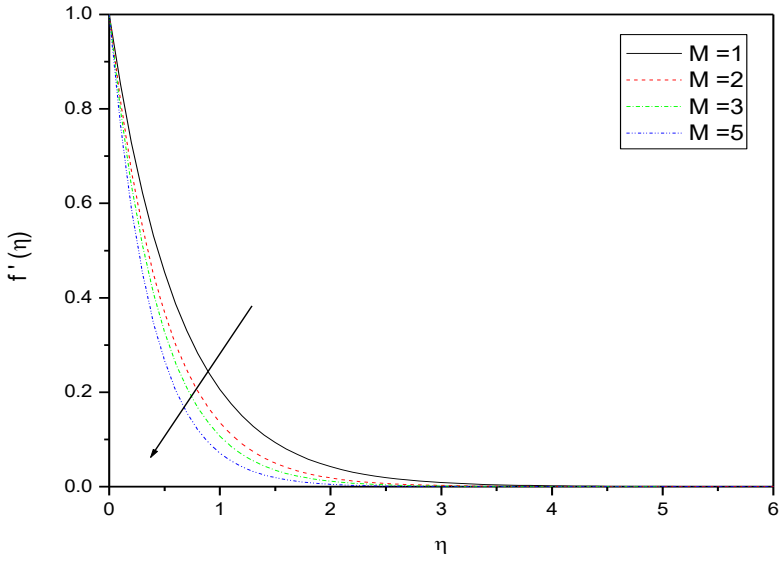

Figure 3. Vertical variation of M when porous parameter K=1 and $R = -0.3$

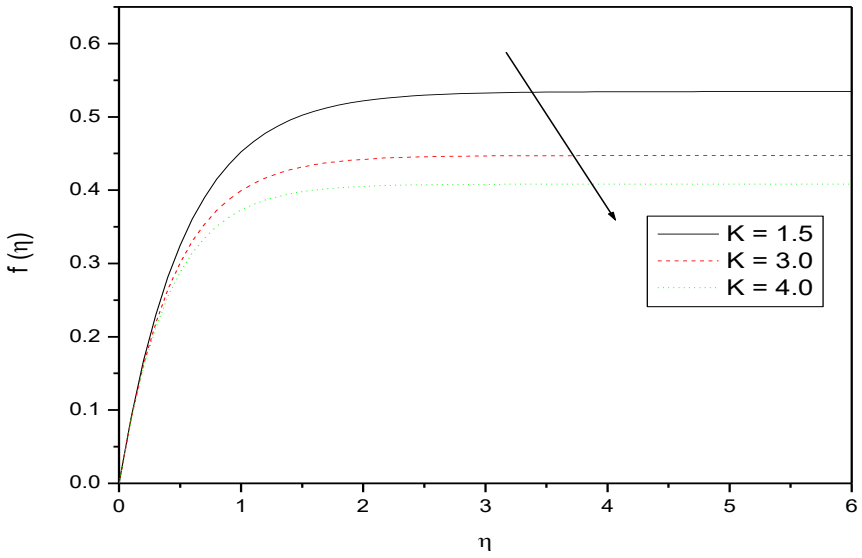

Figure 4. Horizontal variation of K when Magnetic parameter M=1 and $R = -0.3$

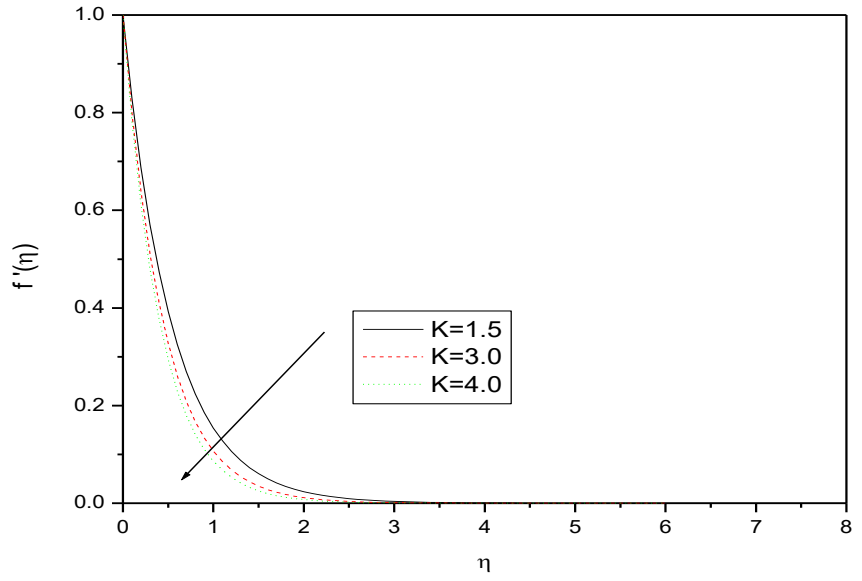

Figure 5. Vertical variation of K when Magnetic parameter M=1

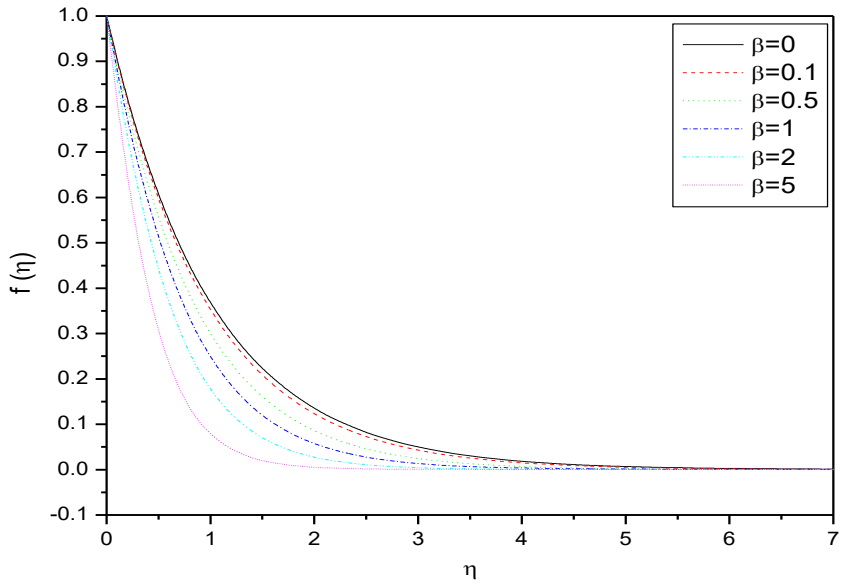

Figure 6. Horizontal Variation of β

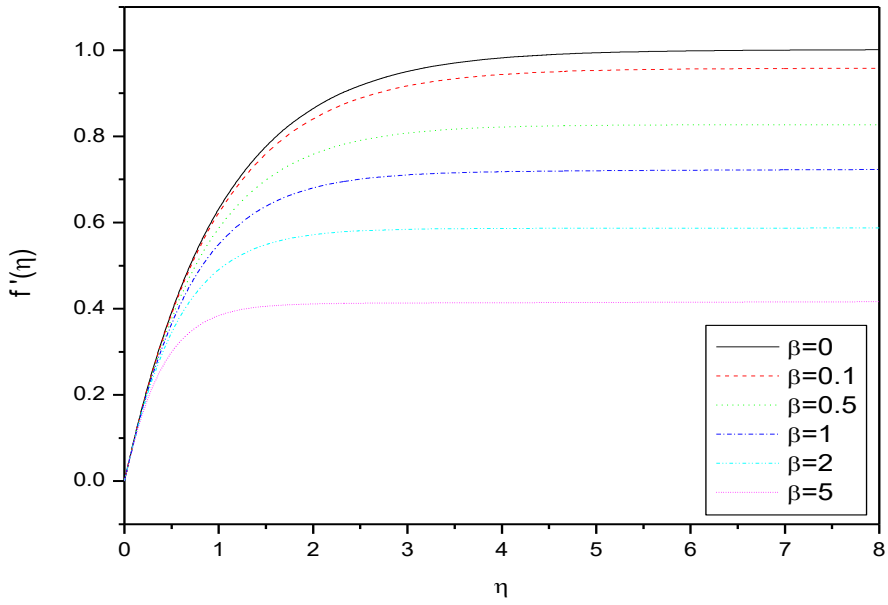

Figure7. Vertical variation of β

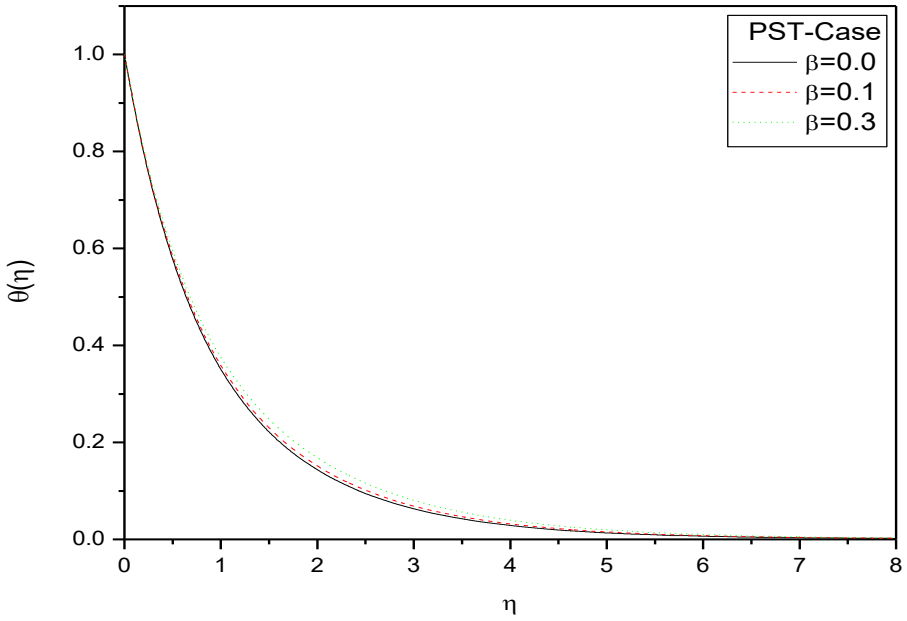

Figure 8. Variation of β for the PST case at $\Pr = 1.0,\ Ec = 0.2, A^* = B^* = 0.1$

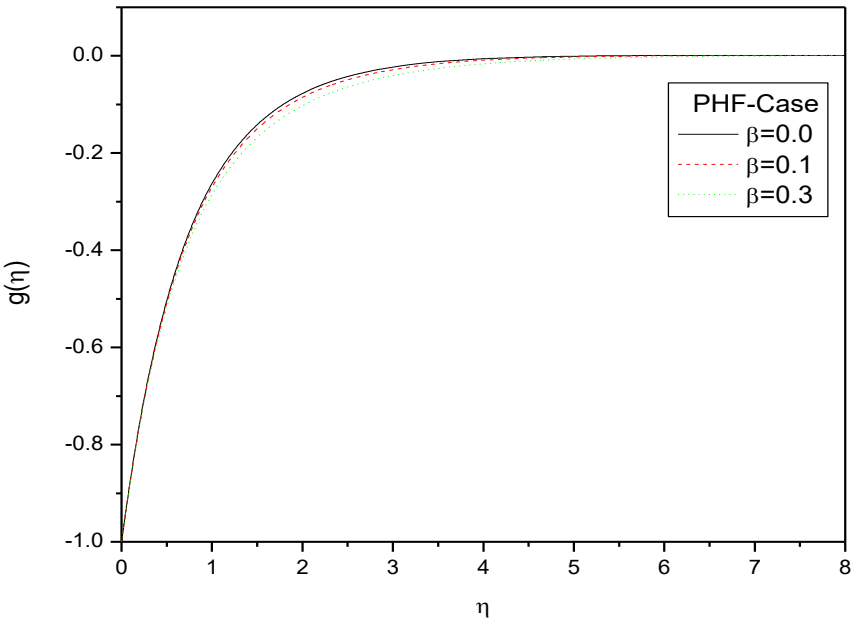

Figure 9. Variation of β for the PHF case at $\Pr = 1.0,\ Ec = 0.2, A^* = B^* = 0.1$

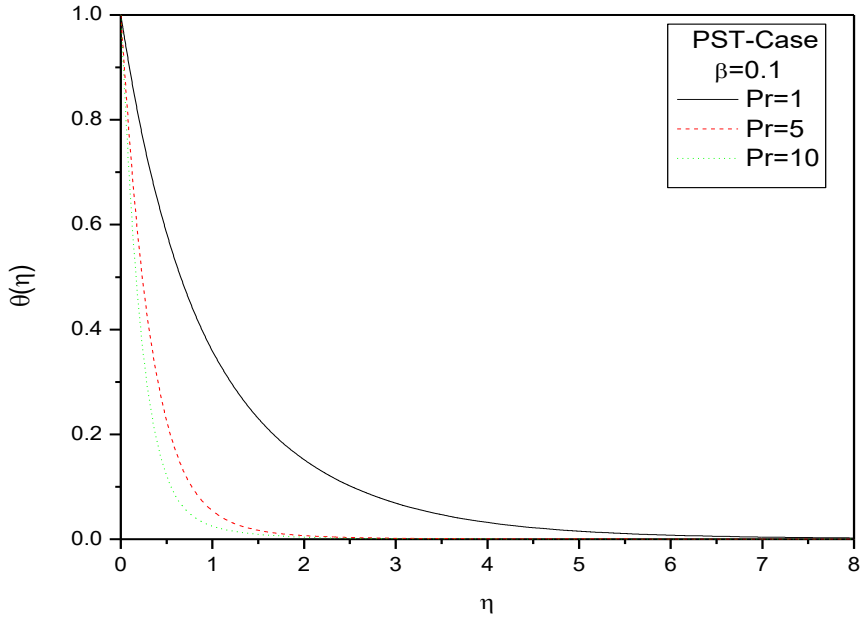

Figure 10. Variation of Pr for the PST case at $\beta = 0.1,\ Ec = 0.2, A^* = B^* = 0.1$

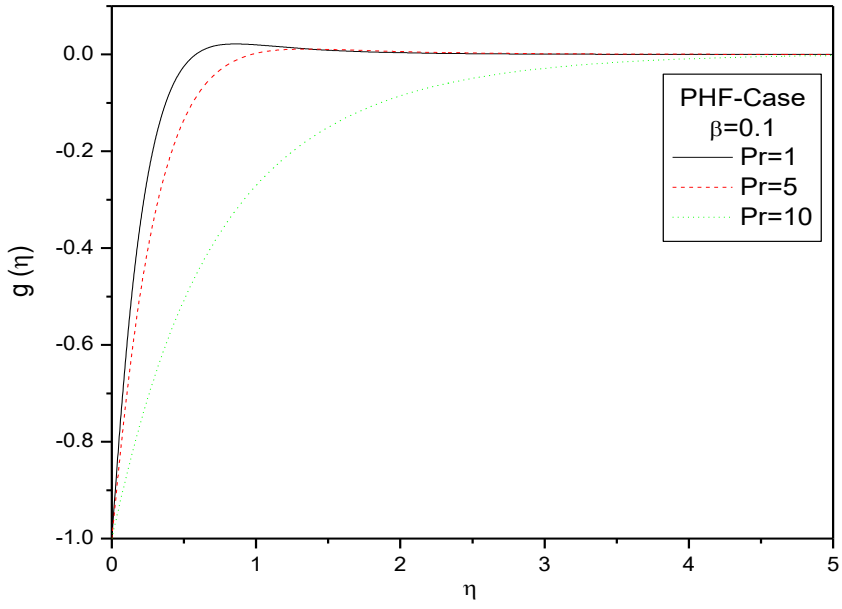

Figure 11. Variation of Pr for the PHF case at $\beta = 0.1, Ec = 0.2, A^* = B^* = 0.1$

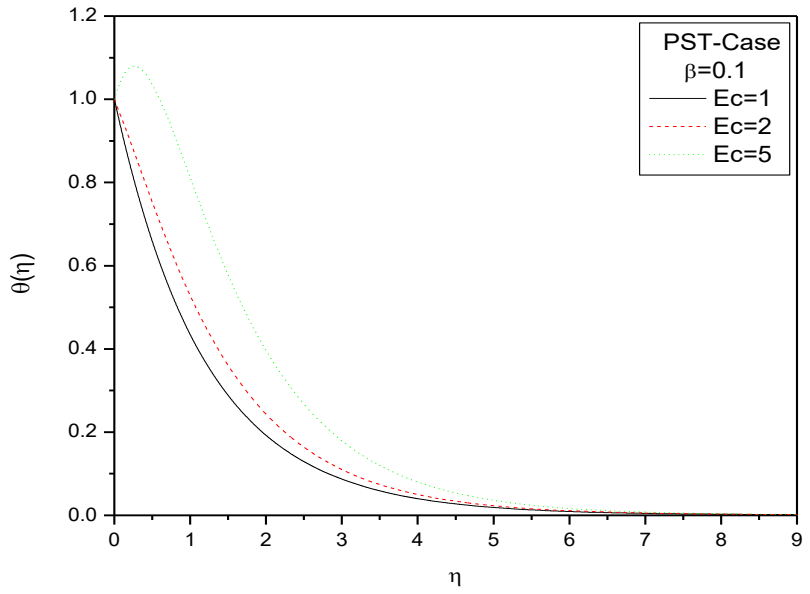

Figure 12. Variation of Ec for the PST case at $\beta = 0.1,\ \mathrm{Pr} = 1, A^* = B^* = 0.1$

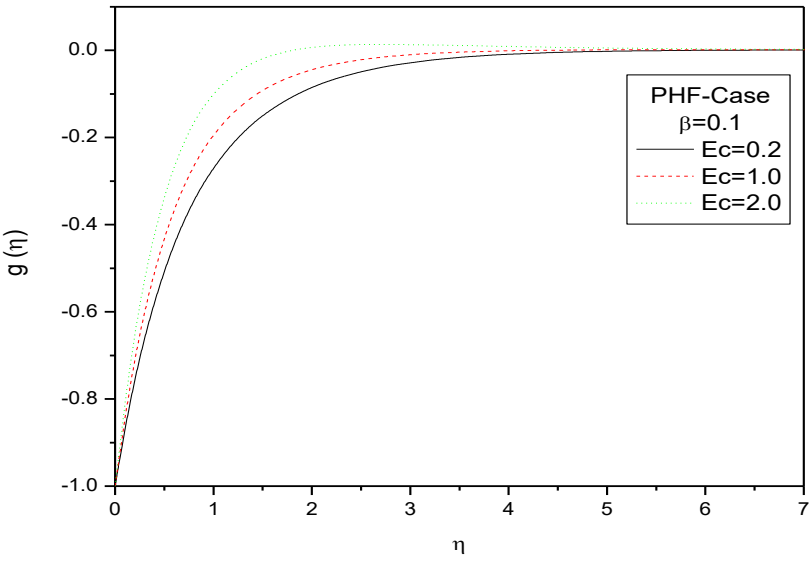

Figure 13. Variation of Ec for the PHF case at $\beta = 0.1,\ \mathrm{Pr} = 1, A^* = B^* = 0.1$

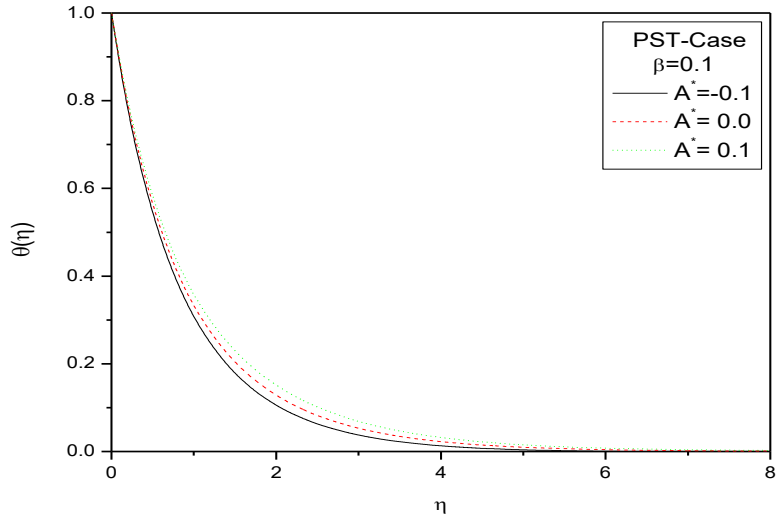

Figure 14. Variation of A* for the PST case at $\beta = 0.1, \mathrm{Pr} = 1, Ec = 0.2, B^* = 0.1$

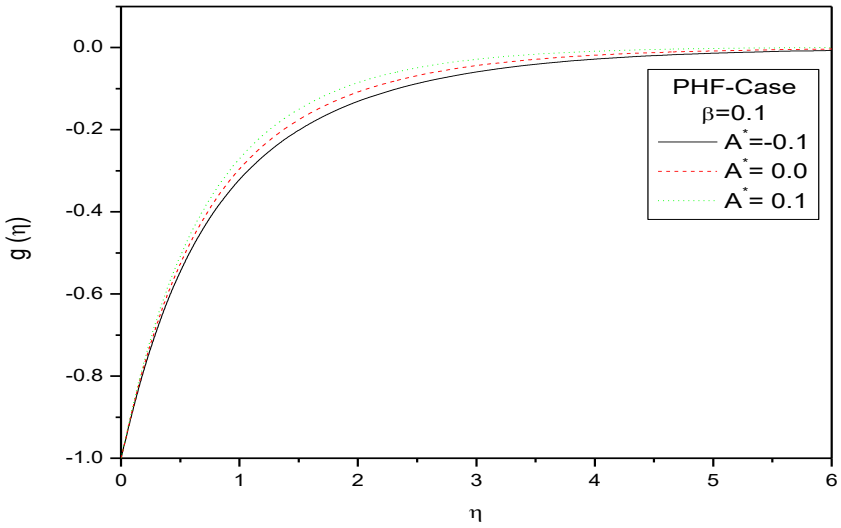

Figure 15. Variation of A* for the PHF case at $\beta = 0.1, \mathrm{Pr} = 1, Ec = 0.2, B^* = 0.1$

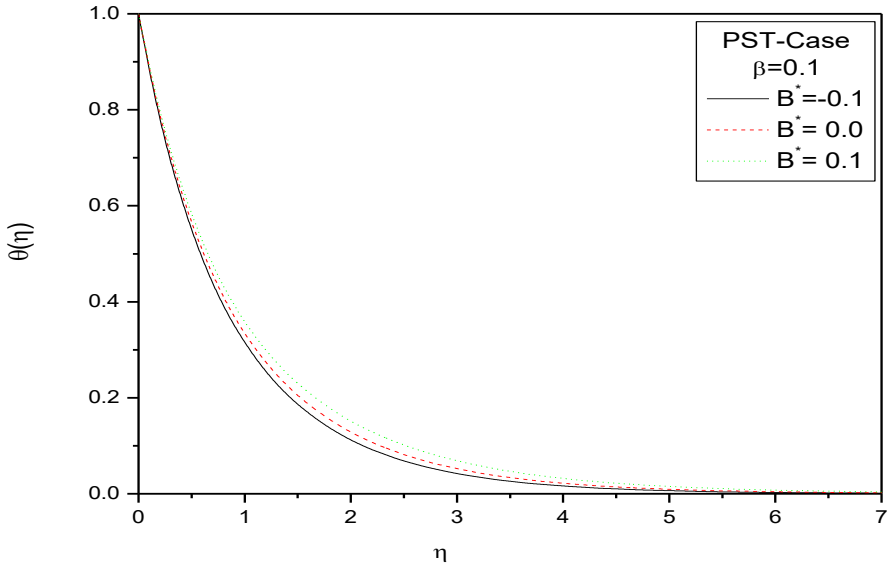

Figure 16. Variation of B* for the PST case at $\beta = 0.1, \mathrm{Pr} = 1, Ec = 0.2, A^* = 0.1$

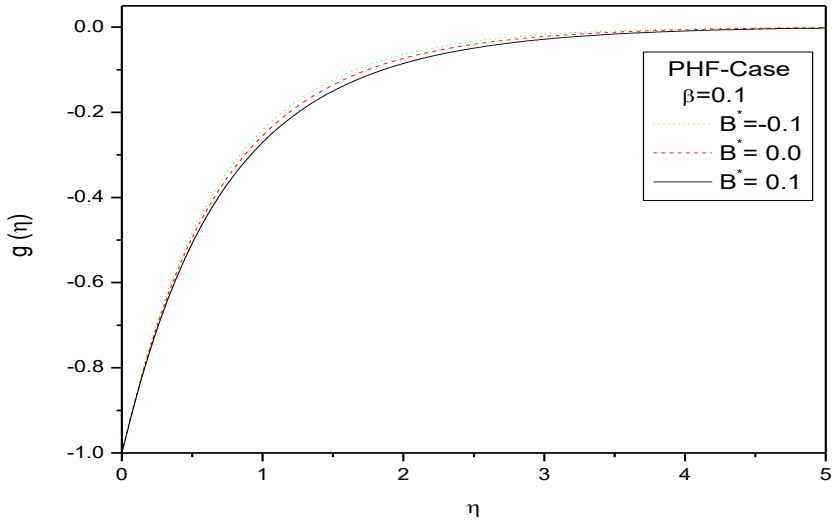

Figure 17. Variation of B* for the PHF case at $\beta = 0.1, \mathrm{Pr} = 1, Ec = 0.2, A^* = 0.1$

Compliance with Ethical Standards:
No conflict exists: The authors declare that we have no conflict of interest.

REFERENCES

1. B.C. Sakiadis, AIChE Journal 7 26-28(1961).
2. L.J. Crane, Journal of Applied Mathematics and Physics (ZAMP) 21, 645-647(1970).
3. C.Y. Wang, *Physics of Fluids*, **31**, 466–468 (1988).
4. C.Y. Wang,Journal of Applied Mathematics and Physics (ZAMP) **39**, 177–185 (1988).
5. P.S. Gupta and A.S. Gupta, *Canadian Journal of Chemical Engineering***55**, 744–746 (1977).
6. T.C. Chiam,*Acta Mechanica***129**, 63–72 (1998).
7. A.A. Pahlavan, V. Aliakbar, F.V. Farahani and K. Sadeghy, Communications in Nonlinear Science and Numerical Simulation 14, 473–488 (2009).
8. A.A. Pahlavan, V. Aliakbar and K. Sadeghy, Communications in Nonlinear Science and Numerical Simulation 14, 779–794 (2009).
9. T. Hayat, Z. Abbas and M. Sajid, Chaos, Solitons and Fractals 39, 840–848 (2009).
10. A.A. Pahlavan, V. Aliakbar, F.V. Farahani, and K. Sadeghy,*Communications in Nonlinear Science and Numerical Simulations***14**, 473–488 (2009).
11. M.S. Abel, J.V.Tawade, M.M.Nandeppanavar, Meccanica 47, 385-393
12. V. Aliakbar, A.A. Pahlavan and K. Sadeghy, Communications in Nonlinear Science and Numerical Simulation*, 14*, 779-794 (2009).
13. K. Sadeghy, H. Hajibeygi andS.M. Taghavi, Int J Non- Linear Mech 41, 1242–1247 (2006).
14. T. Hayat, Z. Abbas andM. Sajid M, Phys Lett A 358, 396–403 (2006)